Reaction Chemistry & Engineering

Catalyst and Reactor Design Considerations for Selective Production of Acids by Oxidative Cleavage of Alkenes and Unsaturated Fatty Acids with H2O2

Journal:	*Reaction Chemistry & Engineering*
Manuscript ID	RE-ART-04-2022-000160.R1
Article Type:	Paper
Date Submitted by the Author:	07-Jun-2022
Complete List of Authors:	Yun, Danim; University of Illinois at Urbana-Champaign, Chemical and Biomolecular Engineering Zhang, Zhongyao; University of Illinois at Urbana-Champaign, Chemical and Biomolecular Engineering Flaherty, David; University of Illinois at Urbana-Champaign, Chemical and Biomolecular Engineering

ARTICLE

Catalyst and Reactor Design Considerations for Selective Production of Acids by Oxidative Cleavage of Alkenes and Unsaturated Fatty Acids with H_2O_2

O,+-----6Received 00th January 20xx,
Accepted 00th January 20xx

DOI: 10.1039/x0xx00000x

Danim Yun, Zhongyao Zhang and David W. Flaherty *

Oxidative cleavage of alkenes and unsaturated fatty acids with hydrogen peroxide gives an efficient and sustainable process to obtain mono- and di-acids for polymers and lubricants with fewer safety risks and less environmental impact than processes that utilize ozone or other inorganic oxidizers (e.g., permanganate, dichromate, etc.). Guided by insight to the mechanisms for competing reaction pathways (i.e., epoxidation of alkene on W-(η^2-O_2) complexes vs. H_2O_2 decomposition) and the apparent kinetics derived from kinetic experiments, here, we postulate that W-based heterogeneous catalysts can provide high performance and stable operations at low H_2O_2 concentrations. Semi-batch reactors with continuous introduction of H_2O_2 solutions offer the means to maintain low H_2O_2 concentrations while providing sufficient quantities of H_2O_2 to satisfy the reaction stoichiometry. We derived simple kinetic model equations for the epoxidation, ring-opening, oxidative cleavage, and oxidation steps and fit theses equations to batch experimental data to obtain kinetic parameters. This kinetic model describes the concentration profiles of reactant, oxidant, and products well as shown by agreement with experimental data. Further predictions of the optimal H_2O_2 feed rate for semi-batch operation utilized by the proposed rate expressions and the reactor design equations suggest that low H_2O_2 feed rate increases selectivity towards oxidative cleavage products and selective use of H_2O_2 for oxidative cleavage pathway. Comparisons of oxidative cleavage of 4-octene in batch and semi-batch reactors show that semibatch reactors with optimized molar feed rates of H_2O_2 increased oxidative cleavage product selectivities (76% to 99%; with an increase in butyric acid selectivity from 1% to 55%) and H_2O_2 selectivity (3% to 30%). In addition, semibatch reaction conditions used avoid H_2O_2-mediated dissolution of W-atoms from the catalyst. Analysis of these findings suggest that solid oxide catalysts will be effective for continuous oxidative cleavage reactions if deployed within fixed-bed reactors that allow for distributed introduction of reactants and therefore low in situ concentrations of H_2O_2.

1. Introduction

Exploring new sources of chemical and energy instead of fossil fuel resources is critical due to concerns regarding depletion of oil resources and environmental problems stemming from fossil fuel usage.[1-3] Biomass valorization is one promising strategy to address this need particularly when a renewable feedstock provides either a drop-in replacement or a functionally advantageous substitute for molecules derived from petroleum.[4, 5] Oxidative cleavage of unsaturated fatty acids (UFAs) obtained from triglycerides or formed by fermentation provides one promising route to replace fossil resources with biomass-derived intermediates, such as through the production of mono- and di-acids from oleic acid (OA).[6, 7] OA is the most abundant naturally occurring fatty acid,[8-10] and the products of oxidative cleavage (i.e., nonanoic acid and azelaic acid) are valuable monomers for synthesis of polyamides and plasticizers.[11-14] Industrially, azelaic acid has been produced by oxidizing OA with ozone generated by passing oxygen through an electrical discharge field,[15] however, this process requires high energy and technologic demand for ozone utilization.[16-19] As an alternative to ozonolysis, oxidative cleavage reactions that utilize nitric acid,[20] permanganate,[21, 22] or dichromate[23] were reported. Yet, these processes are not suitable for practical application due to the toxicity of oxidant and the production of large amounts of harmful gas (*e.g.* N_2O) as a by-product.

Oxidative cleavage of UFAs (and alkenes) with hydrogen peroxide and transition metal-based catalysts avoids these environmental drawbacks. H_2O_2 is less toxic than previously proposed oxidants and only water is a theoretical by-product. In particular, tungsten-based homogeneous and heterogeneous catalysts, including tungstic acid,[24, 25] W-based polyoxometallates,[12, 26-30] and WO_3[16, 31] have been widely reported as active materials for the H_2O_2-mediated oxidative

Department of Chemical and Biomolecular Engineering, University of Illinois Urbana-Champaign, Urbana, IL-61801, USA. Email: dwflhrty@illinois.edu; Tel: +1(217) 244 2816

†Electronic Supplementary Information (ESI) available: Additional information regarding the derivation of reactor design equation, the component generation rate equation, and the rate expressions for the oxidative cleavage of alkene and H_2O_2 decomposition; W leaching test results of WO_x-Al_2O_3; semi-batch prediction results and experimental verifications. See DOI: 10.1039/x0xx00000x

cleavage of alkenes and UFAs. This is because tungsten-based catalysts are inexpensive and non-toxic, and the tungsten peroxo complexes that form *in situ* by reaction with H_2O_2 are highly active for oxidative cleavage compared to those of other transition metals. Benessere et al. reported that the tungstic acid (H_2WO_4) catalyzed reaction of neat OA with aqueous H_2O_2 over tungstic acid (1.45 M OA, 11.6 M H_2O_2, 0.0145 M H_2WO_4, 373 K, 8 h) resulted in an OA conversion greater than 99% with a selectivity of 45% toward azelaic acid.[32] Turnwald et al. reported that peroxo-tris(cetylpyridinium) tungstophosphate (PCWP, H_2O_2-activated (π-$C_5H_5N^+(CH_2)_{15}CH_3)_3(PW_{12}O_{40})^{3-}$) gives 57% azelaic and nonanoic acids yield after the reaction of neat OA with an excess of H_2O_2 (PCWP/OA=0.013, 363 K, 5 h).[26] In comparison, tungsten oxide (WO_3) provides 100% OA conversion with a selectivity of 23% towards azelaic acid with other organic products, *e.g.* nonanoic acid, octanoic acid, nonanal, 9-oxononanoate (0.19 M OA, 2.5 M H_2O_2 in *tert*-butanol, 403 K, 4 h). Additionally, the decomposition of H_2O_2 at above 403 K is rapid during catalysis and notable improvements in azelaic acid selectivity (42%) were observed by adding Na_2SnO_3 as a H_2O_2 stabilizer.[31] Review of these and related results for H_2O_2-mediated oxidative cleavage demonstrates that certain forms of homogeneous catalysts offer high product yields but present challenges for catalyst recovery,[33-35] whereas solid heterogeneous catalysts typically give lower selectivities and yields and lower H_2O_2 selectivity (*i.e.*, the fraction of the amount used for the oxidative cleavage reaction out of the total amount of H_2O_2 consumed). Silica-based matrices and resins have been implemented to bind and hence increase the recyclability of homogeneous complexes such as tungstate (WO_4^{2-}) and phosphotungstate ($H_3PW_{12}O_{40}$)[36, 37] but the weak interaction between these active complexes and the support resulted in catalyst leaching or deactivation. Consequently, we aim to overcome the barriers encountered with heterogeneous catalysts in the oxidative cleavage reactions.

Greater rates, selectivities, and stabilities of heterogeneous catalysts may be achieved through design of improved materials or through use of reaction engineering principles, both of which require mechanistic understanding of the reaction pathways for the desired oxidative cleavage reaction and for undesired H_2O_2 decomposition and catalyst dissolution (i.e., leaching of the active metal). Oxidative cleavage reactions with H_2O_2 over W-based catalysts proceed by reaction of W-peroxo complexes (W-(η^2-O_2))[38-42] with unsaturated substrates to produce epoxides, which sequentially undergo hydrolysis, oxidative cleavage, and oxidation to form acids.[11, 43, 44] W-(η^2-O_2) can also react with an equivalent of H_2O_2 to form molecular oxygen and water (i.e., H_2O_2 decomposition) as shown in scheme 1. Rate expressions we derived for these competing pathways (oxidative cleavage and H_2O_2 decomposition) demonstrate that high molar ratios of the unsaturated organic substrates to H_2O_2 lead to more efficient use of H_2O_2 (i.e., higher H_2O_2 selectivities), which reflects the increased probability that W-(η^2-O_2) encounter the organic reactant at such conditions. These conclusions agree qualitatively with our previous findings for the influence of reactant concentrations on turnover rates and selectivities for H_2O_2-mediated epoxidation of alkenes and competing H_2O_2 decomposition over transition metal substituted zeolites (*e.g.*, Ti-MFI, Ti-BEA, and Nb-BEA)[41, 45-47] and early transition metals grafted onto mesoporous silicates (*e.g.*, Ti-SiO_2, Nb-SiO_2, and Ta-SiO_2).[48, 49] Separately, Fraile *et al.* showed that use of lower H_2O_2 concentrations, achieved by continuous addition of dilute H_2O_2, resulted in greater epoxidation selectivities during reactions of cyclohexene over silica-supported titanium catalysts (2.4 M cyclohexene, 0.24 M H_2O_2 in *tert*-butanol, 353 K, 24 or 11 h for BSTR and SBR, respectively).[50] Wang et al. reported that the epoxide selectivity and the efficiency of H_2O_2 for epoxidation increases by 22% and 10%, respectively, by adding H_2O_2 continuously over 2 h for the epoxidation of styrene with H_2O_2 over Fe-MCM-41 (Si/Fe=86) catalyst (0.8 M styrene, 0.8 M H_2O_2 in dimethylformamide, 346 K, 2 h).[51] Collectively, these mechanistic findings and observations from reactor engineering for epoxidation reactions suggest that use of semi-batch reactors to maintain minimal H_2O_2 concentrations[52, 53] over the course of the oxidative cleavage reaction would increase yields of acid and diacid products and simultaneously increase H_2O_2 selectivity. With sufficient improvements, heterogenous catalysts may provide the basis for viable processes for H_2O_2-mediated oxidative cleavage of alkenes and UFAs.

Here, we compare the performance of homogeneous and heterogeneous tungstate catalysts for H_2O_2-mediated oxidative cleavage reactions and examine the effects of reactant concentrations and reactor design on product yields, H_2O_2 selectivities, and catalyst durability. We use a simple kinetic model developed from the proposed reaction mechanism to estimate kinetic parameters using experimental data derived from batch-stirred tank reactors (BSTR) for the reactions that epoxidize 4-octene, which is a model reactant, ring-open epoxides, oxidatively cleave diols, and oxidize aldehydes to acids. Inspection of these rate expressions and reactor design equations for BSTR and semi-batch reactors (SBR) provides guidance for the optimal reactor model and reactant feed rates. The parameterized model derived from BSTR data agrees well with concentration profiles and performance measured in the SBR (*e.g.*, oxidative cleavage product and H_2O_2 selectivities). These findings show that the SBR operation significantly improved acid and H_2O_2 selectivities from 4 to 55% and 1.5 to 30%, respectively, compared to BSTR operation. The reaction conditions maintaining low [H_2O_2] (< 0.3 mM H_2O_2) during oxidative cleavage increases oxidative cle-

ARTICLE

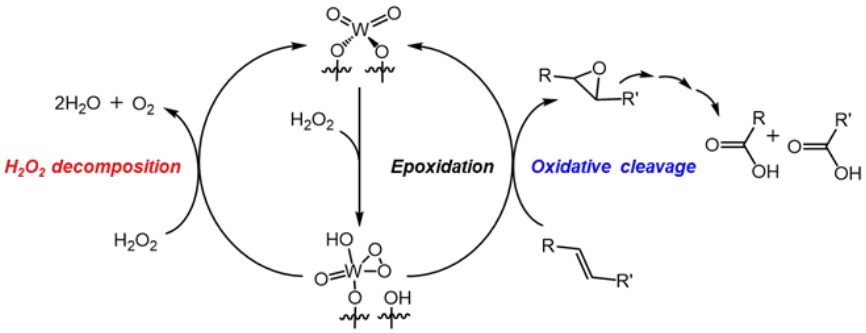

Scheme 1 Reaction scheme of the catalytic oxidative cleavage and H_2O_2 decomposition on the alumina supported tungstate (WO_x-Al_2O_3) catalyst

avage products selectivity while eliminating tungsten leaching from the solid catalysts.

2. Experimental

2.1. Catalyst Synthesis

The tungsten-based heterogeneous (WO_x-Al_2O_3) and homogeneous (tungstic acid and phosphotungstic acid) catalysts were used in this work. In order to obtain WO_x-Al_2O_3 catalyst, the organotungsten complexes ($(C_5H_5)_2$·W·Cl_2, Alfa Aesar, 99%) were grafted on the mesoporous alumina (γ-Al_2O_3, Sigma Aldrich; 3.8 nm pores, 364 $m^2 \cdot g^{-1}$). The procedure is identical to that in our previous research (Supporting Information S1.1).[43] Tungstic acid (H_2WO_4, Sigma-Aldrich, 99%) and phosphotungstic acid hydrate (W-POM; $H_3[P(W_3O_{10})_4]$·xH_2O, Sigma-Aldrich) were purchased and used as received.

2.2. Catalyst Characterization

Energy dispersive X-ray fluorescence (EDXRF) was carried out to determine the composition of the synthesized WO_x-Al_2O_3 catalysts and the quantities of tungsten that leach into solution. Powder or liquid samples were loaded into the He-purged chamber of the spectrometer (EDX-7000, Shimadzu) and scanned from 0 to 30 keV. EDXRF analysis shows that the weight loading of tungsten on WO_x-Al_2O_3 is 4.0%. The areal density of W atoms of the prepared WO_x-Al_2O_3 catalyst is 0.4 W·nm^{-2} as determined by BET surface area calculated from the N_2 adsorption-desoprtion isotherm. In previous work, we found that dehydrated WO_x-Al_2O_3 with 0.4 W·nm^{-2} surface coverage shows Raman features related to ν(W=O), δ(O-W-O), ν(W-O-Al), and WO_3. The results suggest that the WO_x-Al_2O_3 catalyst contains oligomeric tungstate surface species and WO_3 aggregates under dehydrated conditions (SI S1.2).[43]

2.3. Reaction Rate Measurements

BSTR Operation The oxidative cleavage of oleic acid was conducted with neat reactants in batch reactors (100 cm^3, three-neck round-bottom flasks) equipped with a reflux condenser. The cold tap-water was used as a fluid in the condenser. OA (20 mmol, $C_{18}H_{34}O_2$, TCI Chemical, > 99%), and 0.6 g of either a homogeneous (H_2WO_4 and W-POM) or heterogeneous (WO_x-Al_2O_3) catalyst were added to the batch reactor. The mixture (~ 7 cm^3) was heated to 343 K and stirred at 700 rpm for 30 minutes on a stirring hotplate (Corning 6795-420D). The reaction was then initiated by adding 160 mmol aqueous hydrogen peroxide (H_2O_2, Fischer Chemicals, 30% v/v in H_2O). After 17 hours, the reactor was taken out from the oil bath to cool down the temperature. The organic phase was separated from the aqueous phase using a separatory funnel for homogeneous catalysis, and a centrifuge (Eppendorf, Centrifuge 5810 R, 4000 rpm, 30 min, room temperature) for the heterogeneous catalysis.

Oxidative cleavage of 4-octene (trans-4-C_8H_{16}, Sigma-Aldrich, 98%) was conducted in acetonitrile (CH_3CN, Fisher Chemical, ≥ 99.9%) solvent in batch reactors equipped with a reflux condenser. The mixture including 20 mM 4-octene, 50 mg homogeneous or heterogeneous catalyst and acetonitrile was added to the batch reactor. The mixture was heated to 333 K and stirred at 700 rpm for 30 minutes. The reaction was then initiated by adding the 30% v/v aqueous H_2O_2 (0.1 M H_2O_2, 0.39 M H_2O, 30 mL total volume) and continued for 30 minutes. To cease the reaction, the solid catalyst (WO_x-Al_2O_3) was separated by the syringe filter (Tisch Scientific, 0.05 µm, polystyrene) for heterogeneous catalysis and temperature was cooled down to the room temperature for homogeneous catalysis (SI S2.0).

SBR Operation 0.05 M 4-octene, 0.37 g of WO_x-Al_2O_3 catalyst, and 29.8 mL CH_3CN were added to the batch reactor. The mixture was heated to 333 K and stirred at 700 rpm for 30 minutes in a batch reactor equipped with a reflux condenser. The 30% v/v aqueous H_2O_2 was continuously and slowly (F_{H2O2}=1.3, 8.5, or 51 µL min^{-1}) added into the reactor by using a gas tight syringe (Hamilton,

1000 Series, 5 mL) and a syringe pump (KD Scientific, Legato 100). The semi-batch reaction was continued until the desired amount of H_2O_2 (1.53 mL) was added.

Product Analysis For batch and semi-batch reactions, aliquots (~0.6 cm^3) of the reaction solution were extracted as a function of reaction time using a syringe. The concentrations of each compound were analyzed using a gas chromatograph (Agilent 7890A) equipped with a flame ionization detector (FID). Reactants and products were separated in a column (DB-Wax, 60 m x 0.25 mm ID, 0.25 µm film thickness). Peaks within gas chromatograms were identified by comparisons to mixtures of known standards.

The alkene conversion and product yield were calculated as follows:

$$\textbf{Alkene conversion}\ (\%) = \frac{\textit{mole of alkene reacted}}{\textit{mole of alkene fed}} \times \mathbf{100}$$

$$\textbf{Product yield}\ (\%) = \frac{\textit{mole of carbon in product}}{\textit{mole of carbon in alkene fed}} \times \mathbf{100}$$

Oxidative cleavage selectivity (S_{OC} (%)) was calculated as

$$\boldsymbol{S_{OC}}\ (\%) = \frac{\textit{mole of carbon in aldehydes and acids}}{\textit{mole of carbon in all products}} \times \mathbf{100}$$

Colorimetric Titration The concentrations of H_2O_2 in solutions were measured by colorimetric titration. The reaction solution was diluted to 1-10% v/v with CH_3CN. The diluted reaction solution (10 µL) was titrated with an aqueous solution (0.2 cm^3) of $CuSO_4$ (8.3 mM, Fisher Chemicals, >98.6%), neocuproine (12 mM, Sigma-Aldrich, >98%), and ethanol (25% v/v, Decon Laboratories, 100%). The absorbance at 454 nm was determined using a multi-detection microplate reader (Molecular Devices, SpectraMax M5). H_2O_2 selectivity (S_{H2O2} (%)) was calculated as described previously[54]:

$$\boldsymbol{S_{H_2O_2}}(\%) = \frac{\textit{mole of } \boldsymbol{H_2O_2} \textit{ required to form all products observed}}{\textit{mole of } \boldsymbol{H_2O_2} \textit{ consumed}} \times \mathbf{100}$$

2.4. Computational Procedure for the Batch Kinetic Parameters Estimation and Semi-batch Model Prediction

We utilized ideal design equations for BSTR and SBR in the analysis of product concentrations used to estimate kinetic parameters. In the case of the semi-batch reactor, the total liquid volume (V_L) was assumed to additive and a linear function of time:

$$V_L = V_{0L} + V't \qquad (1)$$

where V_{0L} is the initial volume and V' is the volumetric flow rate of the aqueous hydrogen peroxide solution added. Measured concentrations of all species are related to the formation rates of each species i (r_i) by the relationship:

$$\frac{dC_i}{dt} = (C_{0i} - C_i)\frac{V'}{V_L} + r_i\frac{m_{cat}}{V_L} \qquad (2)$$

where C_{0i} and C_i are the initial concentrations and instantaneous concentrations of each component i, respectively, and m_{cat} signifies the mass of the catalyst (see SI S3.1).

In comparison, the liquid volume remains approximately constant (i.e., $V_L=V_{0L}$, $V'=0$) during batch reactions, leading to a simpler design equation (SI S3.1):

$$\frac{dC_i}{dt} = r_i\frac{m_{cat}}{V_{0L}} \qquad (3)$$

The component generation rates (SI S3.2) were inserted in the differential equations (equations (2) and (3)) and these equations were solved numerically with respect to reaction time. The model was implemented in MATLAB R2021a using the ode45 solver for numerical solutions and the algorithm of fmincon in MATLAB was applied for parameter estimation.

3. Results and Discussion

3.1. Comparisons of Tungstate Catalysts for Conversion of Oleic Acid and 4-Octene in Batch Reactors

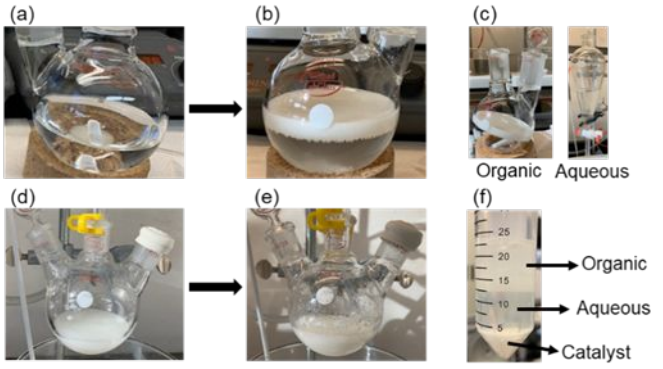

Fig. 1 Appearance of the contents of batch reactors for the oxidative cleavage of oleic acid with H_2O_2 (0.95 M oleic acid, 6.85 M H_2O_2, 27.1 M H_2O, 17 h at 343 K) on (a-c) W-POM and (d-f) WO_x-Al_2O_3. (a,d) Reaction mixture before reaction; (b, e) reaction mixture after reaction at room temperature; (c) organic (left) and aqueous phases (right) of the reaction mixture; (f) three phases of reaction mixture after centrifugation.

Fig. 1 shows images of the contents of the batch reactor before and after the oxidative cleavage of neat oleic acid with H_2O_2 on W-POM and WO_x-Al_2O_3 catalysts (0.95 M oleic acid, 6.85 M H_2O_2, 27.1 M H_2O, 17 h at 343 K) and the materials separated by postreaction processing. After the oxidative cleavage reaction with W-POM catalyst, the reaction mixture separated into organic and aqueous phases. When the temperature decreased to room temperature, the transparent organic phase became an opaque white solid consisting of the organic products resides in the upper layer of the reactor (Fig. 1(b)). The aqueous phase containing the catalyst and residual H_2O_2 was separated from the solid (Fig. 1(c)). For WO_x-Al_2O_3 catalyst, the used catalyst was separated from the reaction mixture (residual reactant, product, residual H_2O_2, and H_2O) by centrifugation (4000 rpm for 30 min), as shown in Fig. 2(f).

The W content of the aqueous and organic phases of the reaction solution for the oleic acid conversion over W-POM were measured by EDXRF (Fig. S4). These spectra indicate that most W species (1.1 mmol, 92%) remain in the aqueous phase, but the organic phase also

contains a small amount of W species (3.2 μmol, 0.3%). These findings typify the challenges with separating homogeneous molecular complexes from the reaction mixture. To overcome this barrier, Benessere *et al*. proposed a method to separate the H_2WO_4 catalyst by adding cold water to quench the reaction and extracting with ethyl acetate to recover the reaction products.[32] The aqueous phase contained the majority of the catalyst as well as residual H_2O_2, and this solution could be combined with additional reactants or evaporated under vacuum to recover the used tungstate catalyst. Consequently, homogeneous catalytic systems for H_2O_2-mediated oxidative cleavage will require similar extraction processes for practical use. In comparison, heterogeneous catalysts are more easily recovered and recycled following oxidative cleavage. While the visible solids are readily recovered, W atoms may leach from the Al_2O_3 support during catalysis. Therefore, we measured the quantity of W-atoms remaining on the Al_2O_3 following contact with H_2O_2 solutions of different concentrations (0.25 – 4 M H_2O_2, 1–16 M H_2O in CH_3CN, 1 h, Fig. S5). The W atom content remains unchanged when $[H_2O_2]$ is less than or equal to 0.25 M, but increasingly, quantities of W atoms leach from the support as $[H_2O_2]$ increases from 0.75 M (10% W lost) to 4.0 M (22% W lost). Thus, the stability of the WO_x-Al_2O_3 catalyst depends strongly on $[H_2O_2]$ and the greatest catalyst stability is anticipated at the lowest values of $[H_2O_2]$ during oxidative cleavage reactions.

Fig. 2a shows turnover numbers for the reactant consumed and the products formed over H_2WO_4, W-POM, and WO_x-Al_2O_3 catalysts for batch reactions of oleic acid, providing a basis to compare the productivities of these homogeneous and heterogeneous catalysts. WO_x-Al_2O_3 gives the highest turnover numbers for oleic acid consumption and epoxide production but the lowest selectivity for oxidative cleavage products (3%; aldehydes and acids) among the three catalysts. Among the homogeneous complexes, H_2WO_4 provides a greater turnover number for oleic acid consumption (12 $mol \cdot mol_W^{-1}$) than W-POM (7.5 $mol \cdot mol_W^{-1}$), but shows significantly lower selectivity for oxidative cleavage products (20%). W-POM gives both the greatest selectivity (85%) and turnover number (5.1 $mol \cdot mol_W^{-1}$) for oxidative cleavage product among the three catalysts under these conditions. 4-Octene was used as a model reactant because oxidative cleavage kinetics and reaction mechanism of oleic acid over WO_x-Al_2O_3 resembles those of 4-octene.[43] The comparisons of turnover numbers for 4-octene consumption and product formation follow similar trends to the turnover numbers in oleic acid conversion (Figure 2). The turnover number for 4-octene consumption shows greater values for the solid catalyst (WO_x-Al_2O_3, 5.3 $mol \cdot mol_W^{-1}$) and much lower values for the homogenous catalysts (0.9 and 0.4 $mol \cdot mol_W^{-1}$ for H_2WO_4 and W-POM, respectively), as shown in Fig. 2(b). Notably, turnover numbers for 4-octene consumption are 10-20 times lower than those for oleic acid, which is due in large part to the lower concentrations used for experiments for 4-octene oxidative cleavage. In addition, W-POM and H_2WO_4 show 16 and 28% H_2O_2 selectivity, respectively, but WO_x-Al_2O_3 shows only 1.5% H_2O_2 selectivity. The low H_2O_2 selectivity of WO_x-Al_2O_3 catalyst indicates that a considerable amount of H_2O_2 is decomposed into water and molecular oxygen on the active sites; the rapid decomposition of H_2O_2 depletes H_2O_2 during the reaction, leading to low oxidative cleavage product selectivity.

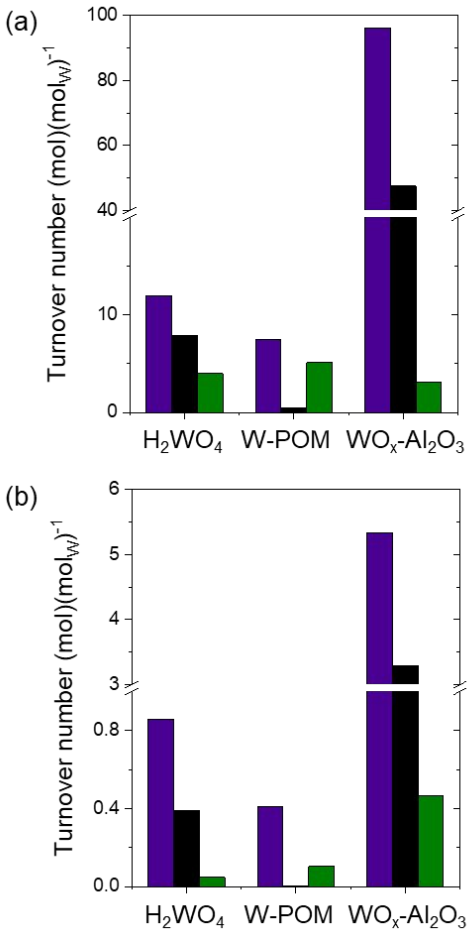

Fig. 2 Turnover numbers for consumed alkenes (■) and formed epoxides (■) and oxidative cleavage products (■, aldehydes and acids) over H_2WO_4, W-POM and WO_x-Al_2O_3 catalysts for the oxidative cleavage of (a) oleic acid (0.95 M oleic acid, 6.85 M H_2O_2, 27.1 M H_2O, 17 h at 343 K), and (b) 4-octene (0.02 M 4-C_8H_{16}, 0.1 M H_2O_2, 0.39 M H_2O in CH_3CN, 0.5 h at 333 K).

To summarize, $[H_2O_2]$ significantly affects the stability of W sites on the Al_2O_3 support, H_2O_2 selectivity, and oxidative cleavage product selectivity. Therefore, we sought fundamental understanding for the importance of $[H_2O_2]$ in oxidative cleavage kinetics over WO_x-Al_2O_3 catalyst and tried to seek optimal reaction conditions for high oxidative cleavage product and H_2O_2 selectivities.

3.2. Kinetic Modelling for BSTR in the Oxidative Cleavage of 4-Octene: from Reaction Mechanism to Rate Expressions

Understanding the reaction mechanism allows us to optimize reaction conditions for the highest yield or selectivity for oxidative cleavage products. As previously discussed, H_2O_2 activates W sites to form W-peroxo complexes (W-(η^2-O_2)).[38-41] These reactive intermediates participate in the kinetically relevant epoxidation step of the oxidative cleavage process. Oxygen atoms from the W-(η^2-O_2) complexes are transferred to alkenes to produce epoxides. Ring opening of epoxides to diols, oxidative cleavage of diols to aldehydes, and further oxidation of aldehydes to acids occur sequentially (Scheme 2). The oxygen transfer step competes with molecular oxygen release, i.e.,

H_2O_2 decomposition. Assuming that oxygen transfer from W-(η^2-O_2) complexes to alkenes is the kinetically relevant step for oxidative cleavage, use of the pseudo steady-state hypothesis on W-(η^2-O_2) complexes leads to complete rate expressions (see S5.1). W-(η^2-O_2) complexes are the most abundant reactive intermediates for both oxygen transfer and H_2O_2 decomposition, leading to the following rate ratio:

$$\frac{r_{OC}}{r_D} = \frac{k_{S4}[4-C_8H_{16}]}{k_{S6}[H_2O_2]} \quad (1)$$

where k_{S4} and k_{S6} are the rate constants for oxidative cleavage (r_{OC}) and H_2O_2 decomposition (r_D), respectively, as shown in Scheme S1. This suggests maintaining low concentration of H_2O_2 ([H_2O_2], where brackets denote the concentration of a species) during catalysis would favor high selectivity for oxidative cleavage products.

Before examining the effects of maintaining low [H_2O_2] on oxidative cleavage rates, we derived simple rate expressions based on the oxidative cleavage mechanism over the WO_x-Al_2O_3 catalyst (Scheme 2). These rate equations explain the concentration profiles of the reactant, intermediates, products, and the oxidant.

The general rate expressions for each of the steps take the following forms:

$$r_1 = k_1[4-C_8H_{16}][H_2O_2-M*] \quad (2)$$

$$r_2 = k_2[4,5-C_8H_{16}O][H_2O] \quad (3)$$

$$r_3 = k_3[4,5-C_8H_{16}(OH)_2][H_2O_2] \quad (4)$$

$$r_4 = k_4[C_3H_7CHO][H_2O_2-M*] \quad (5)$$

$$r_5 = k_5[H_2O_2][H_2O_2-M*] \quad (6)$$

[H_2O_2–M*] is related to the fractional occupancy of H_2O_2-activated metal sites and is determined by the active site requirements for each step reaction. As shown in the supplementary information section 5.2,

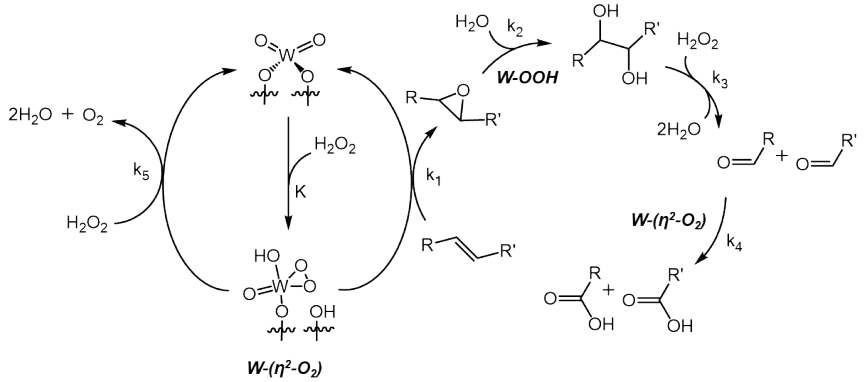

Scheme 2 Stoichiometric reactions involved in the oxidative cleavage of alkenes with H_2O_2 and decomposition of H_2O_2

$$[H_2O_2-M*] = \frac{K_N[H_2O_2]}{1+K_N[H_2O_2]} \quad (7)$$

where K_N is an apparent constant used for brevity that describes how [H_2O_2-M*] depends on [H_2O_2] and implicity contains information regarding the reversibility and rates of all steps that form or consume this shared surface intermediate (SI S5.2 equation S24).

Each step rates for ring opening of 1,2-epoxyoctane, oxidative cleavage of 1,2-octanediol, and H_2O_2 decomposition were measured (see SI S6.0) with each catalyst under various reaction conditions. In the absence of commercially available 4,5-epoxyoctane and 4,5-octanediol at sufficient purities, 1,2-epoxyoctane and 1,2-octanediol were used as surrogates.

Both the epoxidation of 4-octene to 4,5-epoxyoctane and the oxidation of butanal to butyric acid involve oxygen atom transfer from W-(η^2-O_2) complexes.[38-41] Thus, both steps 1 and 4 require the same active W-(η^2-O_2) sites. We derive [W-(η^2-O_2)] as shown in SI S5.3 and use the following rate expressions for steps 1 and 4, respectively:

$$r_1 = k_1[4-C_8H_{16}]\frac{K_6[H_2O_2]}{1+K_6[H_2O_2]} \quad (8)$$

$$r_4 = k_4[C_3H_7CHO]\frac{K_6[H_2O_2]}{1+K_6[H_2O_2]} \quad (9)$$

Figure S7 shows the initial rates for the ring opening of 1,2-epoxyoctane with aqueous H_2O_2 or in the absence of H_2O_2 on WO_x-Al_2O_3 catalyst (0.5 wt% weight loading of W). The ring opening of 1,2-epoxyoctane does not show measurable rates in the absence of H_2O_2, which suggests ring opening rates depend on the concentration of H_2O_2-activated W sites, rather than on the concentration of water.

$$r_2 = k_2[4,5-C_8H_{16}O][W-(\eta^2-O_2)] \quad (10)$$

Brønsted acid sites are known to be active sites for the ring opening of epoxides, and W-peroxo (W-(η^2-O_2)) complexes equilibrate to form W-hydroperoxo (W-OOH) complexes.[55, 56] W-OOH complexes, therefore, are plausible active sites for this step. The fractional occupancy of W-OOH sites can be derived as shown in SI S5.4, and we obtain the following rate expression for step 2:

$$r_2 = k_2[4,5-C_8H_{16}O]\frac{K_7[H_2O_2]}{1+K_7[H_2O_2]} \quad (11)$$

Figure S8 shows oxidative cleavage rates of 1,2-octanediol as a function of [H_2O_2], based on the rates of heptanal and heptanoic acid formations. The measured rates do not depend on the presence of the catalyst, suggesting that this reaction is performed by liquid H_2O_2 in aqueous CH_3CN. This agrees with

proposals by Venturello *et al.*,[57] in which diol cleavage proceeds through an alpha-hydroxy ketone intermediate whose C-C bond is cleaved by nucleophilic attack of H_2O_2. The measured rates do not depend on [H_2O_2], which means that alpha-hydroxy ketone intermediate formation is the kinetically relevant step for 1,2-octanediol oxidative cleavage. Thus, we obtain the following rate expression for step 3:

$$r_3 = k_3[4,5 - C_8H_{16}(OH)_2] \quad (12)$$

Figure S9 shows turnover rates for H_2O_2 decomposition on γ-Al_2O_3 and WO_x-Al_2O_3 (0.5 wt% weight loading of W) catalysts. The measured rates show that γ-Al_2O_3 and WO_x-Al_2O_3 both decomposes H_2O_2 into water and molecular oxygen, which suggests that H_2O_2-activated metal (either W or Al) sites are promising active sites for step 5. We obtain, therefore, the following rate expression for step 5:

$$r_5 = k_5[H_2O_2]\frac{K_8[H_2O_2]}{1 + K_8[H_2O_2]} \quad (13)$$

Collectively, we demonstrated the various types of catalytic sites which participate in oxidative cleavage of alkenes based on the rate comparisons (SI S6.0), and derived simplified rate expressions (equations 8-13) for each step. The kinetic parameters of these expressions (k_1-k_5 and K_6-K_8) are estimated using nonlinear regression as described below (Section 3.3).

3.3. Kinetic Parameter Estimation for the Oxidative Cleavage of 4-Octene over WO_x-Al_2O_3

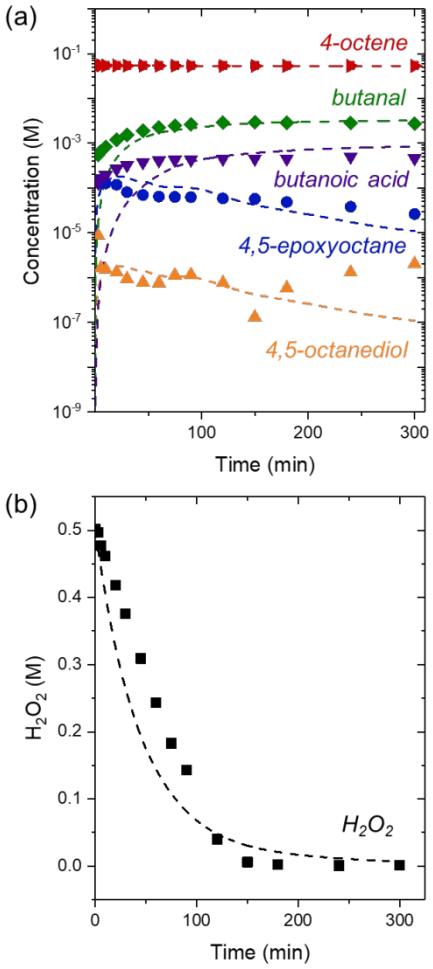

Fig. 3 Concentrations of species during oxidative cleavage of 4-octene (0.05 M 4-octene, 0.5 M H_2O_2, 1.98 M H_2O in CH_3CN at 333 K) over WO_x-Al_2O_3; (a) 4-octene (▶), 4,5-epoxyoctane (●), 4,5-octanediol (▲), butanal (◆) and butyric acid (▼); and (b) H_2O_2 (■). Dashed lines represent model fits.

Fitting the component concentrations obtained from kinetic and reactor models under BSTR operation to experimental data provides kinetic constants for each step (k_i and K_i in equations 8-13). Table 1 shows the kinetic constants obtained from the model, and the standard error of regression (SER, Table 2), the parity plot, and residual plot (Figure S10) indicates the accuracy of our prediction towards experimental data. As shown in Figure S10 and Table 2, the model describes the experimental data well with high accuracy (SER ≤ 0.066). During the parameter estimation, it was noticed that ring opening of 4,5-epoxyoctane, oxidative cleavage of 4,5-octanediol, and butanal oxidation occur fast, but epoxidation of 4-octene occurs slowly. This suggests that epoxidation is the kinetically relevant step for oxidative cleavage. These results corroborate experimental observations.[43] The concentration of 4-octene decreased from 55 mM to 53 mM, while the concentration of butanal increased from 0 mM to 3 mM over the course of a 5 h reaction. In comparison, the [H_2O_2] decreased rapidly from 0.5 M to 0.0 M within 2.5 h. The initial rates for octene consumption, butanal formation, and H_2O_2

formation are 0.08, 0.07, and 2 μmol s^{-1}, respectively. Thus, H_2O_2 decomposition rate is 25-28 times faster than the alkene consumption and butanal formation rates. These rate comparisons demonstrate that the WO_x-Al_2O_3 catalyst suffers from low H_2O_2 selectivities at these reactant concentrations in a BSTR. As a results of the high H_2O_2 decomposition rate, oxidative cleavage of 4-octene ceases after 2.5 h due to total depletion of H_2O_2.

Limiting [H_2O_2] is expected to raise H_2O_2 selectivity and minimize H_2O_2 decomposition by maintaining a high [alkene]/[H_2O_2] ratio. This can be reasonably achieved using a semi-batch system, in which a small amount of H_2O_2 is gradually charged to the reactor. We examine the effects of semi-batch operation on the selectivities of H_2O_2 and oxidative cleavage products and suggest an optimal H_2O_2 feed rate using predictive model based on the proposed rate expressions and reactor design equations (Section 3.4).

3.4. Prediction and Experimental Verification of Oxidative Cleavage Products and H_2O_2 Selectivities as a Function of H_2O_2 Feed Rate in the Semi-batch Operation for the Oxidative Cleavage of 4-Octene

We applied the obtained kinetic parameters and initial concentrations of reactant, oxidant, and products to predict product and H_2O_2 selectivities for the semi-batch operation and compared these to the experimental results. Figure 4 shows that the model predicts experimental results well. Decreasing F_{H2O2} from 51 to 1.3 μL min^{-1} increases oxidative cleavage product and H_2O_2 selectivities. We can see a significant error, however, for butanal and butyric acid selectivities between the experimental values and modeling results (Fig. S11). This means a good fit was accomplished, except for the error in the estimation of butanal oxidation to butyric acid. This was also illustrated in the parity plot, as shown in Figure S10. **These errors in the kinetic parameters for oxidation step may attributable to several factors. First, the most abundant reactive intermediate (MARI) for the oxidation reaction may be different under BSTR and SBR conditions, and the simplified equation (equation (9)) may not explain every case adequately. For BSTR operation, [H_2O_2] is usually higher than [butanal], and H_2O_2-derived species is likely the MARI at this condition. On the other hand, [H_2O_2] may be smaller than [butanal] under SBR operation; thus, adsorbed butanal may be the MARI. In this case, turnover rate for the oxidation step should have 0^{th}-order dependence on [butanal]. This difference may lead to errors in estimations of butanal and butyric acid selectivities.**

Table 1 Estimated rate and equilibrium constants for catalytic oxidative cleavage of 4-octene.

	k_1	k_2	k_3	k_4	k_5	K_6	K_7	K_8
Estimated values	2.8	502	50000	38.5	110	5000	50000	1000

Units: k_1-k_5= L $g^{-1}min^{-1}$; K_6-K_8= L mol^{-1}

Table 2 Standard Error of Regression (SER) between the prediction and experimental results shown in Fig. 3.

	4-Octene	4,5-Epoxyoctane	4,5-Octanediol	Butanal	Butyric acid	H_2O_2
SER[a)]	3.25 x 10^{-4}	4.6 x 10^{-5}	2.28 x 10^{-6}	5.08 x 10^{-4}	2.17 x 10^{-4}	6.62 x 10^{-2}

[a)] $SER = \sqrt{\frac{\sum(C_{exp} - C_{predicted})^2}{n}}$

Second, there may be different active sites which are not considered in the kinetic model of **the oxidation step. Previous studies indicate that hydroxide ions (HO^-), either in solution or at the solution/metal interface, facilitate elementary steps in alcohol oxidation in aqueous media.[58] Kulik et al. reported that a basic environment formed by the addition of NaOH in the presence of Au/Al_2O_3 catalyst gives the highest azelaic acid (86%) and nonanoic acid (99%) yields by the oxidative cleavage of 9,10-dihydroxystearic acid with molecular oxygen.[59] They suggest HO^- is produced during the formation and dissociation of peroxide, acting as an active site under the reaction conditions. Under batch operation, liquid H_2O_2 is insufficient for further oxidation due to rapid H_2O_2 decomposition, while semi-batch operation enables the oxidation of butanal with liquid H_2O_2 or HO- formed by formation of peroxide complexes on metal or in the solution. This can lead to different butanal oxidation rates in BSTR and SBR operation. Third, the concentrations of water differ between each mode of operation (and as a function of time during SBR) may influence rates and product selectivities. The presence of different quantities of water on the surface near the active site may affect the stability of transition states and hence rates constants, which would lead to changes in turnover rates.[45, 60, 61] Al_2O_3 surfaces possess surface hydroxyl groups that may bind water and facilitate these changes. In addition, water can be adsorbed on the catalyst surface,[62-64] leading to the structural transformation and alteration of the catalytic capabilities. BSTR operation provides large amount of water and can have a high probability of transformation in the active site to non-active. Collectively, these assumptions may lead to errors in the model predictions of selectivities of butanal and butyric acid. Overall, however, the model explains the kinetics of oxidative cleavage of 4-octene with H_2O_2 well under BSTR and SB operation.**

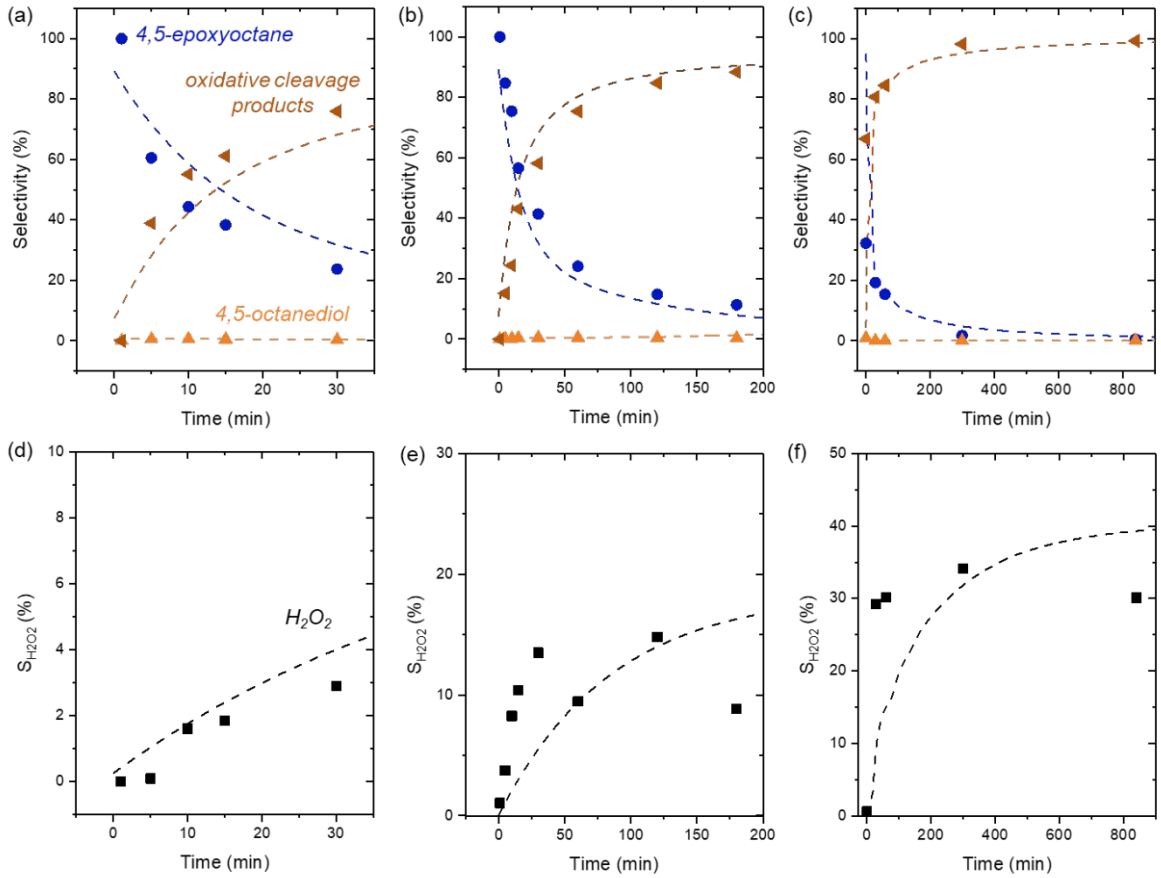

Fig. 4 Selectivities toward products formed by reactions of 4-octene and H2O2 as a function of time in semibatch conditions on WO_x-Al_2O_3 catalyst (0.05 M 4-octene in CH_3CN at 333 K). (a-c) Selectivities among organic products (4,5-epoxyoctane (●), 4,5-octanediol (▲), and oxidative cleavage products (◀; butanal and butyric acid)), and (d-f) selectivity for H_2O_2 (■) ((a,d) F_{H2O2}=51 μL min^{-1}, (b,e) F_{H2O2}=8.5 μL min^{-1}, and (c,f) F_{H2O2}=1.3 μL min^{-1}). Dashed lines signify model predictions.

Our prediction also provides the optimal H_2O_2 feed rate (F_{H2O2}) for high oxidative cleavage product selectivity under SBR operation. As shown in Figure 5, decrease of F_{H2O2} from 51 to 1.3 μL min^{-1} in the SBR operations gives 1.3-fold (from 76 to 99%) increase in oxidative cleavage product and 10-fold increase (from 2.9 to 30%) in H_2O_2 selectivities. Moreover, the SBR operation for the oxidative cleavage of 4-octene with the optimal F_{H2O2} (1.3 μL min^{-1}) improved the oxidative cleavage products selectivity (>99%, and 55% to butyric acid, specifically (Fig. S11)) with and H_2O_2 selectivity equal to 30%, compared to that BSTR operation provides 71% oxidative cleavage products selectivity (4% to butyric acid selectivity) and 1.5% H_2O_2 selectivity. In addition, WO_x-Al_2O_3 catalysts are stable and regenerable during semibatch operation, which was established by conducting four subsequent batch reactions, each followed by an oxidative catalyst regeneration treatment (SI S4.3). The W content of the regenerated catalyst was determined by EDXRF and compared to that of the fresh catalyst. Figure S6 shows that 9.4% of W leaches from the support after BSTR operation (50 mM 4-octene, 0.5 M H_2O_2, 1.98 M H_2O in CH_3CN, 333K), while W does not leach from the Al_2O_3 after SBR operation (50 mM 4-octene in CH_3CN, 333K, F_{H2O2}=1.3 μL min^{-1}). The turnover numbers slightly decrease (~7%) after three sequential BSTR operation, but turnover numbers consistently maintain for all three semibatch reactions. This demonstrates that the WO_x-Al_2O_3 catalysts are stable and regenerable during semibatch operation. Collectively, SBR operation improved the oxidative cleavage selectivity and catalyst stability by maintaining a high [4-octene]/[H_2O_2] ratio because the small amount of H_2O_2 during a reaction not only kinetically favors oxidative cleavage rather than H_2O_2 decomposition but also prohibits W leaching.

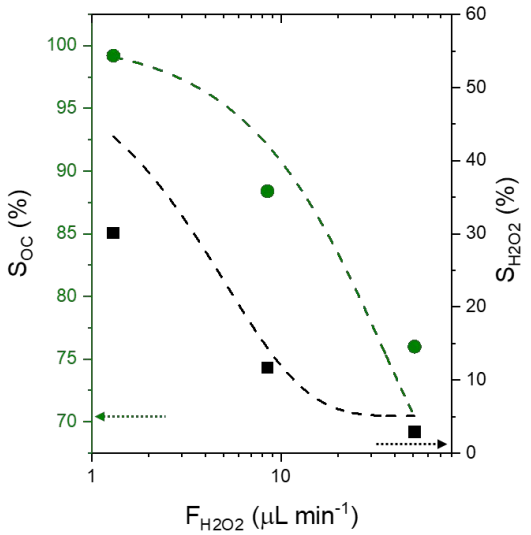

Fig. 5 Selectivities toward oxidative cleavage products (butanal and butyric acid, ●, —) and H_2O_2 (■, —) during oxidative cleavage of 4-octene (0.05 M 4-octene in CH_3CN at 333 K) as functions of H_2O_2 feed rate over WO_x-Al_2O_3. The black and blue arrows indicate selectivities toward oxidative cleavage products and H_2O_2 selectivity measured in the BSTR (0.05 M 4-octene, 0.5 M H_2O_2, 1.98 M H_2O in CH_3CN at 333 K). Dashed lines signify model predictions using parameters from Table 1.

4. Conclusions

We compared rates and selectivities for oxidative cleavage of oleic acid and 4-octene over homogeneous (H_2WO_4 and W-POM) and heterogeneous (WO_x-Al_2O_3) catalysts. Under BSTR operation, the homogeneous W-POM catalyst shows the highest selectivities toward oxidative cleavage products (aldehydes and acids, 85 and 94% in the reactions of oleic acid and 4-octene, respectively) among the three catalysts, but additional techniques are required to separate spent catalyst from the reaction mixture. On the other hand, WO_x-Al_2O_3 shows the lowest oxidative cleavage product selectivities (3 and 7% for aldehydes and acids in the reaction of oleic acid and 4-octene, respectively), but the used catalyst can be easily separated from the reaction mixture by centrifugation. WO_x-Al_2O_3 shows low H_2O_2 selectivity (1.5%) compared to W-POM (28%) and H_2WO_4 (16%) in the oxidative cleavage of 4-octene, which means H_2O_2 decomposes rapidly on WO_x-Al_2O_3 during catalysis. Additionally, low [H_2O_2] (< 0.25 M) minimizes loss of W-atoms from the solid catalyst. The kinetic results suggest the ratio of the rates for two competing reactions, oxidative cleavage of alkene and H_2O_2 decomposition, depends on the ratios of [alkene] to [H_2O_2]. Therefore, maintaining low [H_2O_2] during catalysis is critical to obtain high oxidative cleavage products and H_2O_2 selectivities and stability of the solid catalyst.

SBR operation offers an opportunity to maintain values for [alkene] to [H_2O_2] that are low during the reaction while satisfying the stoichiometric requirements of the reaction. The gradual introduction of H_2O_2 significantly increases oxidative cleavage products and H_2O_2 selectivities compared to BSTR operation. In the BSTR, oxidative cleavage of 4-octene gave 71% oxidative cleavage products selectivity and 1.5% H_2O_2 selectivity. On the other hand, the optimized reaction conditions for the SBR gives 99% selectivity to oxidative cleavage products with 30% H_2O_2 selectivity. To predict the optimal H_2O_2 feed rate for SBR operation, a kinetic model based on simplified rate expressions for each step in the oxidative cleavage under BSTR condition and reactor model equations were used. The proposed kinetic model describes the component concentration profiles of oxidative cleavage during catalysis well as shown by agreement with experimental data. Further model predictions of optimal F_{H2O2} for oxidative cleavage suggest that low F_{H2O2} increases oxidative cleavage and H_2O_2 selectivities. Experimentally, a 40-fold decrease in F_{H2O2} during SBR operation improved 1.3-fold and 10-fold increase in oxidative cleavage products (76% to 99%; with an increase in butyric acid selectivity from 1% to 55%) and H_2O_2 selectivities (2.9% to 30%), respectively. Collectively, the results from experiments and modeling show that SBR operation with continuous introduction of dilute [H_2O_2] significantly greater selectivities and improved stability of the WO_x-Al_2O_3 catalyst. This work suggests that SBR may enable other oxidation processes that intend to valorize biomass utilization and produce renewable chemicals.

Author Contributions

All authors have given approval to the final version of the manuscript.

Conflicts of interest

There are no conflicts to declare.

Acknowledgements

This work was funded by the DOE Center for Advanced Bioenergy and Bioproducts Innovation (U.S. Department of Energy, Office of Science, Office of Biological and Environmental Research under Award Number DE-SC0018420). Any opinions, findings, and conclusions or recommendations expressed in this publication are those of the author(s) and do not necessarily reflect the views of the U.S. Department of Energy. EDXRF was carried out in the Frederick Seitz Materials Research Laboratory at the University of Illinois. We thank Vijay M. Shah for careful review of this manuscript.

Notes and References

1. F. Cherubini, *Energy Conversion and Management*, 2010, **51**, 1412-1421.
2. J. Sepulveda, S. Teixeira and U. Schuchardt, *Applied Catalysis A: General*, 2007, **318**, 213-217.
3. C. O. Tuck, E. Pérez, I. T. Horváth, R. A. Sheldon and M. Poliakoff, *Science*, 2012, **337**, 695-699.
4. H. Kargbo, J. S. Harris and A. N. Phan, *Renewable and Sustainable Energy Reviews*, 2021, **135**, 110168.
5. W. H. Faveere, S. Van Praet, B. Vermeeren, K. N. R. Dumoleijn, K. Moonen, E. Taarning and B. F. Sels, *Angewandte Chemie International Edition*, 2021, **60**, 12204-12223.

6. U. Biermann, U. T. Bornscheuer, I. Feussner, M. A. R. Meier and J. O. Metzger, *Angewandte Chemie International Edition*, 2021, **60**, 20144-20165.
7. S. Gámez, E. de la Torre and E. M. Gaigneaux, *Chemical Engineering Journal*, 2022, **427**, 131820.
8. M. M. Rhead, G. Eglinton, G. H. Draffan and P. J. England, *Nature*, 1971, **232**, 327-330.
9. T. Akcan, R. Gökçe, M. Asensio, M. Estévez and D. Morcuende, *Journal of food science and technology*, 2017, **54**, 3050-3057.
10. R. H. Glew, F. A. Ayaz, C. Sanz, D. VanderJagt, H. Huang, L. Chuang and M. Strnad, *European Food Research and Technology*, 2003, **216**, 390-394.
11. P. Spannring, P. C. Bruijnincx, B. M. Weckhuysen and R. J. K. Gebbink, *Catalysis Science & Technology*, 2014, **4**, 2182-2209.
12. A. Godard, P. De Caro, S. Thiebaud-Roux, E. Vedrenne and Z. Mouloungui, *Journal of the American Oil Chemists' Society*, 2013, **90**, 133-140.
13. G. A. D. L. Izeppi, J.-L. Dubois, A. Balle and A. Soutelo-Maria, *Industrial Crops and Products*, 2020, **150**, 112411.
14. F. Zimmermann, E. Meux, J.-L. Mieloszynski, J.-M. Lecuire and N. Oget, *Tetrahedron Letters*, 2005, **46**, 3201-3203.
15. A. C. B. Charles G. Goebel, Herman F. Oehischlaeger, and Richard P. Rolfes,, *US2813113*, 1953.
16. H. Noureddini and M. Kanabur, *Journal of the American Oil Chemists' Society*, 1999, **76**, 305-312.
17. A. Behr, N. Tenhumberg and A. Wintzer, *RSC advances*, 2013, **3**, 172-180.
18. T. Cousin, G. Chatel, N. Kardos, B. Andrioletti and M. Draye, *Catalysis Science & Technology*, 2019, **9**, 5256-5278.
19. P. Spannring, V. Yazerski, P. C. Bruijnincx, B. M. Weckhuysen and R. J. K. Gebbink, *Chemistry–a European Journal*, 2013, **19**, 15012-15018.
20. F. O. Ayorinde, G. Osman, R. L. Shepard and F. T. Powers, *Journal of the American Oil Chemists' Society*, 1988, **65**, 1774-1777.
21. N. Garti and E. Avni, *Colloids and Surfaces*, 1982, **4**, 33-41.
22. I. Garti and E. Avni, *Journal of the American Oil Chemists' Society*, 1981, **58**, 840-841.
23. M. Ansell, I. Shepherd and B. Weedon, *Journal of the Chemical Society C: Organic*, 1971, 1840-1846.
24. M. A. Oakley, S. Woodward, K. Coupland, D. Parker and C. Temple-Heald, *Journal of Molecular Catalysis A: Chemical*, 1999, **150**, 105-111.
25. M. Rüsch, G. Klaas, P. Bavaj and S. Warwel, *Lipid/Fett*, 1995, **97**, 359-367.
26. S. Turnwald, M. Lorier, L. Wright and M. Mucalo, *Journal of materials science letters*, 1998, **17**, 1305-1307.
27. Z. Pai, A. Tolstikov, P. Berdnikova, G. Kustova, T. Khlebnikova, N. Selivanova, A. Shangina and V. Kostrovskii, *Russian chemical bulletin*, 2005, **54**, 1847-1854.
28. T. B. Khlebnikova, Z. P. Pai, L. A. Fedoseeva and Y. V. Mattsat, *Reaction Kinetics and Catalysis Letters*, 2009, **98**, 9-17.
29. E. Antonelli, R. D'Aloisio, M. Gambaro, T. Fiorani and C. Venturello, *The Journal of Organic Chemistry*, 1998, **63**, 7190-7206.
30. A. Haimov, H. Cohen and R. Neumann, *Journal of the American Chemical Society*, 2004, **126**, 11762-11763.
31. X. Li, J. Choo Ping Syong and Y. Zhang, *Green Chemistry*, 2018, **20**, 3619-3624.
32. V. Benessere, M. E. Cucciolito, A. De Santis, M. Di Serio, R. Esposito, F. Ruffo and R. Turco, *Journal of the American Oil Chemists' Society*, 2015, **92**, 1701-1707.
33. J. H. Clark and D. J. Macquarrie, *Chemical Society Reviews*, 1996, **25**, 303-310.
34. H. P. Dijkstra, G. P. M. van Klink and G. van Koten, *Accounts of Chemical Research*, 2002, **35**, 798-810.
35. in *Organometallic Chemistry and Catalysis*, ed. D. Astruc, Springer Berlin Heidelberg, Berlin, Heidelberg, 2007, DOI: 10.1007/978-3-540-46129-6_16, pp. 351-355.
36. P. Levecque, H. Poelman, P. Jacobs, D. De Vos and B. Sels, *Physical Chemistry Chemical Physics*, 2009, **11**, 2964-2975.
37. Y. M. A. Yamada, *Chemical and Pharmaceutical Bulletin*, 2005, **53**, 723-739.
38. M. Amini, M. M. Haghdoost and M. Bagherzadeh, *Coordination Chemistry Reviews*, 2014, **268**, 83-100.
39. A. Arcoria, F. P. Ballistreri, G. A. Tomaselli, F. Di Furia and G. Modena, *The Journal of Organic Chemistry*, 1986, **51**, 2374-2376.
40. H. Mimoun, *Journal of Molecular Catalysis*, 1980, **7**, 1-29.
41. E. Z. Ayla, D. S. Potts, D. T. Bregante and D. W. Flaherty, *ACS Catalysis*, 2021, **11**, 139-154.
42. E. Z. Ayla, D. S. Potts, D. T. Bregante and D. W. Flaherty, *ACS Catalysis*, 2020, **11**, 139-154.
43. D. Yun, E. Z. Ayla, D. T. Bregante and D. W. Flaherty, *ACS Catalysis*, 2021, **11**, 3137-3152.
44. A. E. Kerenkan, F. Béland and T.-O. Do, *Catalysis Science & Technology*, 2016, **6**, 971-987.
45. D. T. Bregante, M. C. Chan, J. Z. Tan, E. Z. Ayla, C. P. Nicholas, D. Shukla and D. W. Flaherty, *Nature Catalysis*, 2021, **4**, 797-808.
46. J. Z. Tan, D. T. Bregante, C. Torres and D. W. Flaherty, *Journal of Catalysis*, 2022, **405**, 91-104.
47. D. T. Bregante, P. Priyadarshini and D. W. Flaherty, *Journal of Catalysis*, 2017, **348**, 75-89.
48. D. T. Bregante, J. Z. Tan, A. Sutrisno and D. W. Flaherty, *Catalysis Science & Technology*, 2020, **10**, 635-647.
49. D. T. Bregante, N. E. Thornburg, J. M. Notestein and D. W. Flaherty, *ACS Catalysis*, 2018, **8**, 2995-3010.
50. J. M. Fraile, J. I. Garćia, J. A. Mayoral and E. Vispe, *Applied Catalysis A: General*, 2003, **245**, 363-376.
51. Y. Wang, Q. Zhang, T. Shishido and K. Takehira, *Journal of Catalysis*, 2002, **209**, 186-196.
52. W. Y. Perez-Sena, J. Wärnå, K. Eränen, P. Tolvanen, L. Estel, S. Leveneur and T. Salmi, *Chemical Engineering Science*, 2021, **230**, 116206.
53. J. Wu, J. Bewtra, N. Biswas and K. Taylor, *The Canadian Journal of Chemical Engineering*, 1994, **72**, 881-886.
54. L. H. Callanan, R. M. Burton, J. Mullineux, J. M. M. Engelbrecht and U. Rau, *Chemical Engineering Journal*, 2012, **180**, 255-262.
55. D. T. Bregante and D. W. Flaherty, *Journal of the American Chemical Society*, 2017, **139**, 6888-6898.
56. P. Jin, D. Wei, Y. Wen, M. Luo, X. Wang and M. Tang, *Journal of Molecular Structure*, 2011, **992**, 19-26.
57. C. Venturello and M. Ricci, *The Journal of Organic Chemistry*, 1986, **51**, 1599-1602.
58. B. N. Zope, D. D. Hibbitts, M. Neurock and R. J. Davis, *Science*, 2010, **330**, 74-78.
59. A. Kulik, A. Janz, M.-M. Pohl, A. Martin and A. Köckritz, *European Journal of Lipid Science and Technology*, 2012, **114**, 1327-1332.

60. D. S. Potts, D. T. Bregante, J. S. Adams, C. Torres and D. W. Flaherty, *Chemical Society Reviews*, 2021, **50**, 12308-12337.
61. D. T. Bregante and D. W. Flaherty, *ACS Catalysis*, 2019, **9**, 10951-10962.
62. D. Mandelli, M. C. A. van Vliet, R. A. Sheldon and U. Schuchardt, *Applied Catalysis A: General*, 2001, **219**, 209-213.
63. G. Lefèvre, M. Duc, P. Lepeut, R. Caplain and M. Fédoroff, *Langmuir*, 2002, **18**, 7530-7537.
64. A. I. Osman, J. K. Abu-Dahrieh, D. W. Rooney, J. Thompson, S. A. Halawy and M. A. Mohamed, *J Chem Technol Biotechnol*, 2017, **92**, 2952-2962.